Title
Mechanisms of laser-induced thermal coagulation of whole blood in vitro

Authors
Pfefer, T Joshua
Choi, Bernard
Vargas, Gracie
et al.

Publication Date
1999-06-22

DOI
10.1117/12.350970

Mechanisms of Laser-Induced Thermal Coagulation of Whole Blood *in vitro*

T. Joshua Pfefer*, Bernard Choi, Gracie Vargas, Karen M. McNally and A. J. Welch

Biomedical Engineering Program, The University of Texas at Austin,
Austin, Texas 78712 USA

ABSTRACT

Quantitative data regarding photothermal and damage processes during pulsed laser irradiation of blood are necessary to achieve a better understanding of laser treatment of cutaneous vascular lesions and improve numerical models. In this study, multiple experimental techniques were employed to quantify the effects of single-pulse KTP laser (λ = 532 nm, τ_p = 10 ms) irradiation of whole blood *in vitro*: high-speed temperature measurement with a thermal camera in line-scan mode (8 kHz); optical coherence tomography (for determination of coagulum morphology); and transmission measurement with a co-aligned laser beam (λ = 635 nm). Threshold radiant exposures for coagulation (4.4-5.0 J/cm^2) and ablation (~12 J/cm^2) were identified. Thermal camera measurements indicated threshold coagulation temperatures of 90-100 °C, and peak temperatures of up to 145 °C for sub-ablation radiant exposures. Significant changes in coagulum thickness and consistency, and a corresponding decrease in transmission, were observed with increasing radiant exposure. The Arrhenius equation was shown to produce accurate predictions of coagulation onset (using appropriate rate process coefficients). The significance of dynamic effects such as evaporative loss and dynamic changes in optical properties was indicated. Implications for numerical modeling are discussed. Most importantly, the threshold temperatures typically quoted in the literature for pulsed laser coagulation (60-70 °C) and ablation (100 °C) of blood do not match the results of this study.

Keywords: Arrhenius equation, blood, heat transfer, KTP laser, optical coherence tomography, temperature measurement, thermal damage, vaporization.

1. INTRODUCTION

Thermal coagulation of blood constituents plays a significant role in therapeutic laser applications such as treatment of cutaneous vascular lesions[1] and tissue welding.[2] However, there remains a lack of quantitative data regarding the optical and thermal mechanisms of laser coagulation of blood, particularly for pulsed laser irradiation.

Laser-induced vessel destruction, or photothermolysis, typically involves the absorption of light by hemoglobin in blood, the diffusion of heat into the surrounding vessel wall and dermis, and thermal damage of blood constituents and/or endothelial cells. In recent studies using optical coherence tomography (OCT)[3] and confocal microscopy,[4] pulsed laser irradiation has been shown to produce coagula in the lumen of cutaneous vessels *in vivo*. As radiant exposure (H_o) levels increase, these coagula become larger and cause vessel occlusion and necrosis. These results, and the inability of present optical-thermal models to predict them, underscore the need for a greater understanding of the mechanisms of thermal damage in blood.

1.1 Thermal coagulation of blood constituents *in vitro*

For the purposes of this study, whole blood can be viewed as a non-homogeneous protein solution. Blood plasma is comprised primarily of water (91%) and proteins (7%, 7.3 gm/dL) such as albumin (4.5 gm/dL) and globulin (2.5 g/dL).[5,6] The primary protein component of the erythrocytes is hemoglobin (14-16 gm/dL of whole blood), although a smaller quantity of proteins such as spectrin comprise the cell membranes.

* Correspondence: Email: pfefer@mail.utexas.edu ; WWW: http://www.ece.utexas.edu/projects/bell ;
Telephone: (512) 471-4703; Fax: (512) 475-8854

Part of the SPIE Conference on Cutaneous Applications of Lasers: Dermatology, Plastic Surgery, and Tissue Welding • San Jose, California • January 1999
SPIE Vol. 3590 • 0277-786X/99/$10.00

Thermally-induced biochemical and morphological effects have been investigated previously. As blood is exposed to heat, the normally biconcave red blood cell assumes a biconvex shape, then forms a spherocyte.[7] Partial membrane fragmentation occurs, resulting in a loss of hemoglobin. Finally, the membrane disintegrates into globules which aggregate to form a mesh, and the release of hemoglobin is completed.[8,9] The thermal damage to the membrane is attributed to conformational changes in erythrocyte membrane structural proteins.[10] Whether or not membrane protein coagula represent a significant volume of flow-stopping coagula has not been determined. However, these changes have been noted to induce a small increase in scattering and absorption at λ = 633 nm.[7]

Several *in vitro* studies have involved continuous wave (CW) irradiation of whole blood, blood constituents, or phantoms. Early studies investigated the effect of CW argon laser radiation on morphological changes in erythrocytes and the release of hemoglobin[8,11]. Flock *et al.*[12] used various lasers to heat red blood cell solutions and assessed damage via measurements of free hemoglobin. Using an Arrhenius rate process analysis, the authors argued that the chemical process of erythrocyte membrane damage is different depending on the rate at which energy is delivered (and thus governed by different rate process coefficients). However, the study's methods were different for different heating rates: a water bath and direct thermal measurements for low rates versus laser heating and theoretically predicted temperatures for high rates. Halldorsson recorded temperatures with a thermal camera during CW Nd:YAG laser irradiation of whole blood.[13] A decrease in the rate of temperature rise seen near 60 °C was attributed to convective and evaporative losses. A decrease in transmission that occurred near 70 °C was attributed to two thermal effects: de-oxygenation of hemoglobin which produced an increase in absorption; and denaturation which produced an increase in scattering. It was also concluded that water vaporization led to the production of solid coagula found in the blood.

Recent studies have investigated the effects of pulsed laser irradiation on whole blood or similar protein-rich biological solutions *in vitro*. Verkryusse *et al.*[14] documented changes in transmission and reflection of pulsed dye laser light (λ = 586 nm), which they attributed to temperature-dependent changes in absorption. The authors concluded that scattering effects were negligible, despite observations that coagulation onset brought about a decrease in transmission and the appearance of a "whitish disk". Other recent studies have documented the transient development of pulsed Holmium:YAG (λ = 2.12 μm, τ_p = 0.13-1.0 ms) laser-induced coagulation in albumen - essentially a water-ovalbumin (86%-14%) solution - using fast flash photography.[15,16] In these experiments, thermal damage produced an increase in light scattering and a coagulum which, for higher radiant exposures, adhered to the optical fiber tip.

1.2 The Arrhenius Equation

The standard method of quantifying thermal damage in biological tissue is the Arrhenius rate process equation:[17-19]

$$\Omega(t) = \ln\left(\frac{C(0)}{C(t)}\right) = A\int_0^t \exp\left(-\frac{E_a}{RT}\right)d\tau \qquad (1)$$

where T is temperature (Kelvin), t is time (seconds), A is the frequency factor (1/s) and E_a is the activation energy (J/mole) of the reaction, C is the concentration of living cells or molecules in the native state, and R is the universal gas constant (8.31 J/mole/°K). The damage threshold for tissue necrosis is Ω = 1.0 (when 63 % of the material has been thermally altered). This threshold corresponds with the visual onset of coagulation, usually noted as an increase in scattering, or whitening.[20] Rate process coefficients for blood constituents, bulk skin and arterial tissue are presented in Table 1, along with the threshold temperatures for coagulation, given a one-millisecond exposure duration and step changes in temperature. The relationship between threshold temperatures and exposure time is displayed in Figure 1, for selected data from Table 1. These rate process coefficients were obtained using exposure durations on the order of hundreds of milliseconds or greater. Therefore, the high threshold temperatures predicted for pulse durations of 10 ms or less represent a significant extrapolation of experimental data, the validity of which has not been established previously.

Researchers have generally assumed threshold blood coagulation temperatures of 60-70 °C in their theoretical models of laser treatment of vascular lesions.[21,22] These values have been based on studies performed with continuous wave lasers, as well as data from Henriques' study of bulk skin burns from 1947,[17] which are commonly cited in the literature.[23,24] Therefore, it is the goal of this study to investigate the veracity of these assumptions through quantification of the thermal and optical effects of pulsed laser-induced irradiation of blood.

Table 1: Arrhenius rate process coefficients of blood constituents and related biological materials and corresponding threshold temperatures for an exposure duration of 10 ms.

Material	A (1/s)	E_a (kJ/mole)	T_{th} (°C) for τ=10 ms	Reference
Albumen	3.8 E57	385	89	Yang *et al.*[20]
Bovine serum albumin	3.2 E56	379	90	McNally[25]
Erythrocyte membrane	8.3 E42	289	96	Lepock *et al.*[10]
Erythrocyte membrane	6.8 E36	249	160	Moussa *et al.*[26]
Hemoglobin	7.6 E66	455	93	Lepock *et al.*[10]
Hemoglobin	7.6 E76	550	100	Barnes[27]
Bulk Skin	3.1 E98	628	67	Henriques[17]
Aorta	5.6 E63	430	91	Agah *et al.*[28]

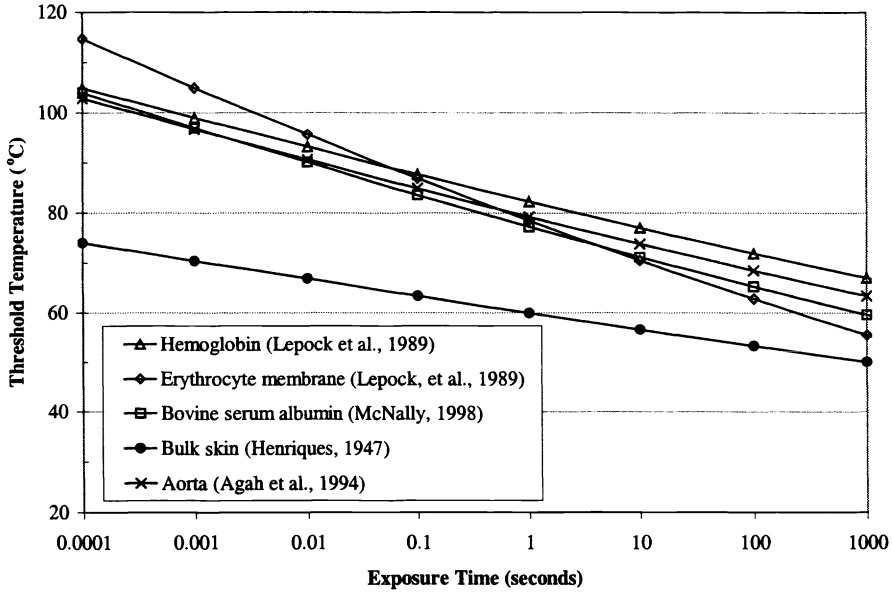

Figure 1: Threshold temperatures of skin and blood constituents as a function of exposure time, using rate process data in Table 1, and assuming step changes in temperature. Symbols are for identification purposes only and do not represent specific data points.

2. MATERIALS AND METHODS

The experimental portion of this study involved the use of three primary methods: thermal imaging (to measure transient surface temperatures), optical coherence tomography (for documenting coagulum morphology, particularly thickness), and laser transmission measurements. All experiments were performed with a Coherent Versapulse VPW – a clinical KTP (frequency doubled Nd:YAG) laser with a wavelength of 532 nm. A pulse duration (τ_p) of 10 ms and spot sizes of 5 mm (H_o = 2.5-6.0 J/cm^2), 4 mm (H_o = 6.5-7.5 J/cm^2), and 3 mm (H_o = 8.0-13.0 J/cm^2) were used. Human venous blood from a healthy male donor was withdrawn and placed in vials containing the anti-coagulant ethylenediamine tetraacetic acid (EDTA). When necessary, vials were placed in a refrigerator for overnight storage and returned to ambient temperature the next day. All blood was used within 36 hours of withdrawal. Gentle agitation was performed to achieve a homogeneous distribution of blood constituents. For open-cuvette irradiations, blood was mixed in the vial, dispensed to the cuvette and irradiated within 30 seconds. For spectrophotometer (glass) cuvette irradiations, the blood was agitated within the closed cuvette immediately before irradiation. The lack of closed-cuvette experimental data for the highest radiant exposures is due to the fact that ablation events would occasionally cause the glass to fracture.

Data have not been corrected for losses due to specular reflection. For the thermal imaging setup, the handpiece was oriented at an incident angle of ~22° (from perpendicular) and an open cuvette was used (n_{air} = 1.0, n_{blood} = 1.33), thus producing specular reflection of 2.0%. For OCT imaging and transmission measurements, the incident angle was 0°, and a closed cuvette was used, resulting in a specular reflection of 4.3% (air-glass and glass-blood interfaces, where n_{glass} = 1.5).

2.1 Thermal imaging and thermal damage calculations

Temperature measurements were performed using an Inframetrics 600L (λ = 3-5 μm, band-limited) thermal camera. Radiation emitted from the sample (or the blackbody) was reflected off of a standard front-sided mirror to accommodate a horizontally oriented detector. Calibration curves for several temperature ranges were developed using a variable temperature blackbody. The curves maximized the accuracy at high temperatures at the cost of decreased accuracy at lower temperatures when the camera was set for larger temperature ranges (higher H_o events). The spatial resolution of the camera was approximately 0.1 mm. The emissivity of blood was assumed to be that of water (ε = 0.96). Temperature measurements through the center of the beam were taken using line-scan mode. This method provided acquisition of a single line of spatial data at a rate of 8 kHz, providing a temporal resolution of 125 μs. However, line scan mode also introduced several problems which limited the continuity of measurement: the scale bar and time code, which could not be removed, covered up several lines of data; the fly-back of the camera resulted in a loss of 3.5 ms of data every frame (each 33 ms). Thus, transient temperature distributions at the center of the beam were measured in temporal segments and a continuous data set was reconstructed by averaging data from several events.

Quantitative estimation of thermal damage was achieved by evaluating the Arrhenius equation using the experimentally determined temperature data and rate process coefficients for bulk skin[17] and hemoglobin.[10] Numerical integration of this relation was performed at each 125-μs time step using the trapezoidal method.

2.2 Optical Coherence Tomography imaging

An OCT system used in previous studies to image hamster blood vessels *in vivo*[29] was used to determine the macroscopic morphology of the coagulum. The system is essentially a modified Michelson interferometer that measures the intensity of light backscattered from specific locations within the sample. It incorporates a 1280 nm center wavelength superluminescent diode. A single depth-scan is acquired by changing the reference arm length. Scanning mirrors are used to scan the beam laterally across the sample in order to construct a two dimensional cross-sectional image. The OCT system has a high dynamic range (>100dB) and a spatial resolution of 20 μm, both laterally and axially. Blood was enclosed in a glass spectrophotometer cuvette (2 mm sample path length) and irradiated. Immediately after irradiation, the sample was moved to the OCT stage and a two-dimensional image was generated. The acquisition time for an image comprised of 200 depth-scans was approximately 20 seconds.

2.3 Transmission Measurements

Transmission measurements were performed to quantify the effect of laser-induced optical changes. The 2 mm path length glass spectrophotometer cuvette was filled with blood. A photodetector below the cuvette recorded the intensity of the alignment beam (λ = 635 nm). A circular aperture 6 mm in diameter was placed between the cuvette and the photodetector to remove highly scattered light. The output from the photodiode was captured by a digital oscilloscope (Tektronix TDS 640A) and processed on a personal computer. Although a high-pass filter was used to minimize the effect of the KTP laser and flashlamp, the signal from the alignment beam was overwhelmed by stray light during the laser pulse. Therefore, transient data during the pulse was not documented in this study. The development of coagulation produced a decrease in the transmission signal from before to after the laser pulse. These data were transferred by disk from the oscilloscope to a personal computer where the data was stored and analyzed.

3. RESULTS

3.1 Observations during open-cuvette irradiations

As the radiant exposure was increased from 2.5 J/cm^2, no visible changes were noted until 3.6 J/cm^2, when a faint irregular whiteness was seen on the blood surface. At H_o = 4.4 J/cm^2 a thin, light-gray disk about 8 mm in diameter (as compared to the 5 mm spot size) resembling a dusting of fine particles was produced. The disk became irregular as it dispersed, and dissolved when the cuvette was agitated. This disk became increasingly visible, and began to aggregate at a radiant exposure of 8.0 J/cm^2. At H_o = 10 J/cm^2, the coagulum could be removed from the cuvette with forceps as a single piece. Although

occasional ablation events - identified by an audible acoustic transient (popping sound) accompanied by fragmentation of the otherwise disk-shaped coagulum - were noted at H_o = 11 J/cm^2, ablation did not occur consistently until H_o = 13 J/cm^2.

Indications of rapid evaporation were visualized by placing a glass slide suspended about a centimeter above the blood. As the radiant exposure was increased, the first noticeable change (at H_o = 2.7 J/cm^2) was an accumulation of a thin layer of condensation on the slide which appeared soon after the laser pulse and disappeared after a few seconds. The intensity and extent of the water droplet layer increased steadily with H_o. An attempt to quantify mass loss during irradiation using a scale with sensitivity on the order of tens of micrograms was unsuccessful due to a low signal to noise ratio.

3.2 Temperature measurements and damage predictions

The temperature reconstructions for a point near the center of the beam are shown in Figure 2. Each curve represents an average of data from 10-15 irradiations. The standard deviation for points near the temperature peak was +/- 2 °C for H_o = 3 J/cm^2, increasing to +/-5 °C at H_o = 12 J/cm^2. Initially, the rate of temperature rise was proportional to the radiant exposure. For lower radiant exposures (3-5 J/cm^2), this rate did not change significantly unless temperatures exceeded 70 °C. However, for higher radiant exposures (8-12 J/cm^2), deviation from the initial rate of temperature rise did not appear to be significant until temperatures approached 100 °C. The predictions of transient accumulation of thermal damage, as calculated from the temperature data in Figure 2, are presented for bulk skin (Figure 3a) and hemoglobin (Figure 3b) rate process coefficients. As expected, these figures indicate similar trends, yet Figure 3a indicates significantly earlier times of coagulation onset and greater damage levels than Figure 3b.

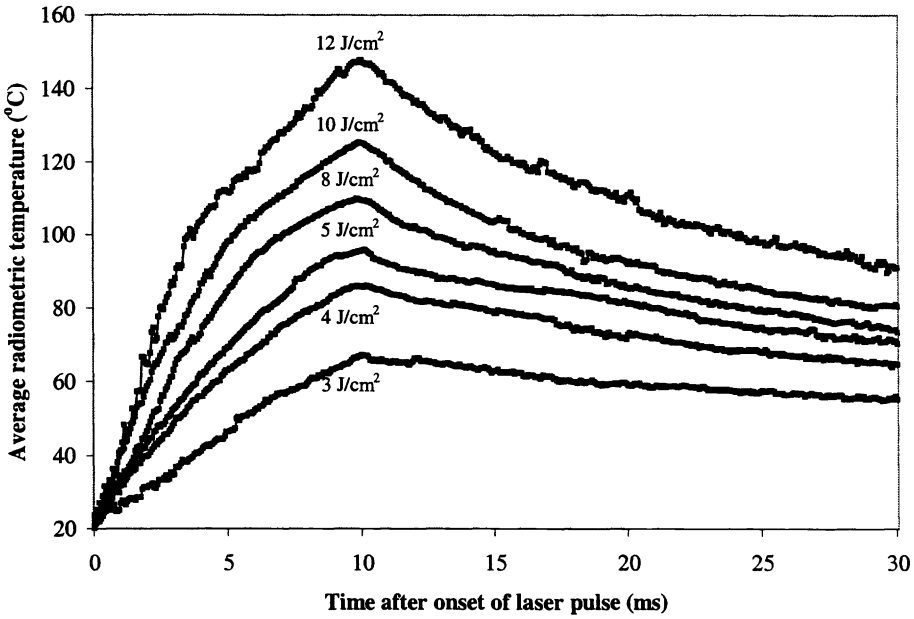

Figure 2: Radiometric temperature distributions for a point near the center of the laser spot for six different radiant exposure levels.

3.3 OCT imaging of coagulum morphology

Figure 4 shows a series of images which document the change in coagulum thickness with increasing radiant exposure. In these images, four layers are visible (as labeled in Figure 4d, from top to bottom): a dark layer of glass, a thin white layer due to the change in index of refraction at the interface between the glass (n = 1.5) and the blood (n = 1.33), a light, speckled region of highly scattering coagulated blood, and a darker speckled region of native blood which extends to the bottom of each image. A sample of 3 to 5 images at each radiant exposure was used to generate the data shown in Figure 5. The first sign of a coagulum occurred at H_o = 4.4 J/cm^2. The initial increase in coagulum thickness was followed by a regime of linear growth in coagulum size with radiant exposure. The signal from the native blood was inversely proportional to the thickness of the coagulum above it, as is apparent in Figure 4d, which shows the lateral edge of a coagulum. Due to the size of the

coagula (<200 μm), the spatial resolution of the OCT system, and the noise level associated with OCT imaging of scattering media, the quantitative data obtained was not highly precise.

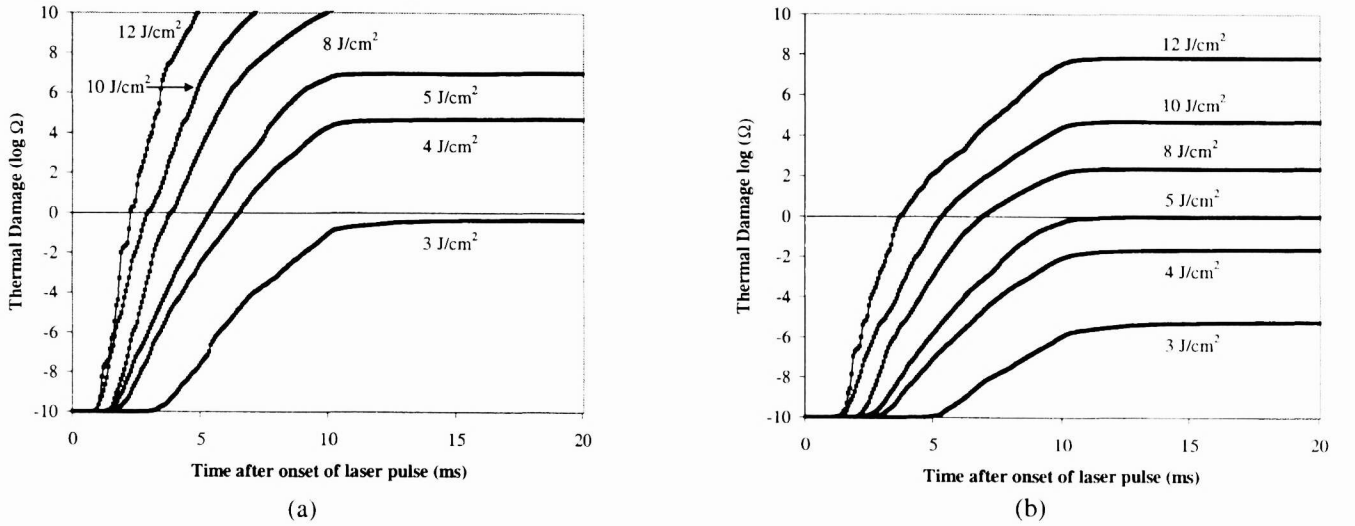

Figure 3: Thermal damage levels calculated from the radiometric temperature distributions in Figure 2 using rate process coefficients (a) for bulk skin[17] and (b) hemoglobin.[10] Note that the minimum and maximum values of Ω (10^{-10} and 10^{10}) were chosen arbitrarily. Horizonal lines at Ω = 1 indicate the damage threshold.

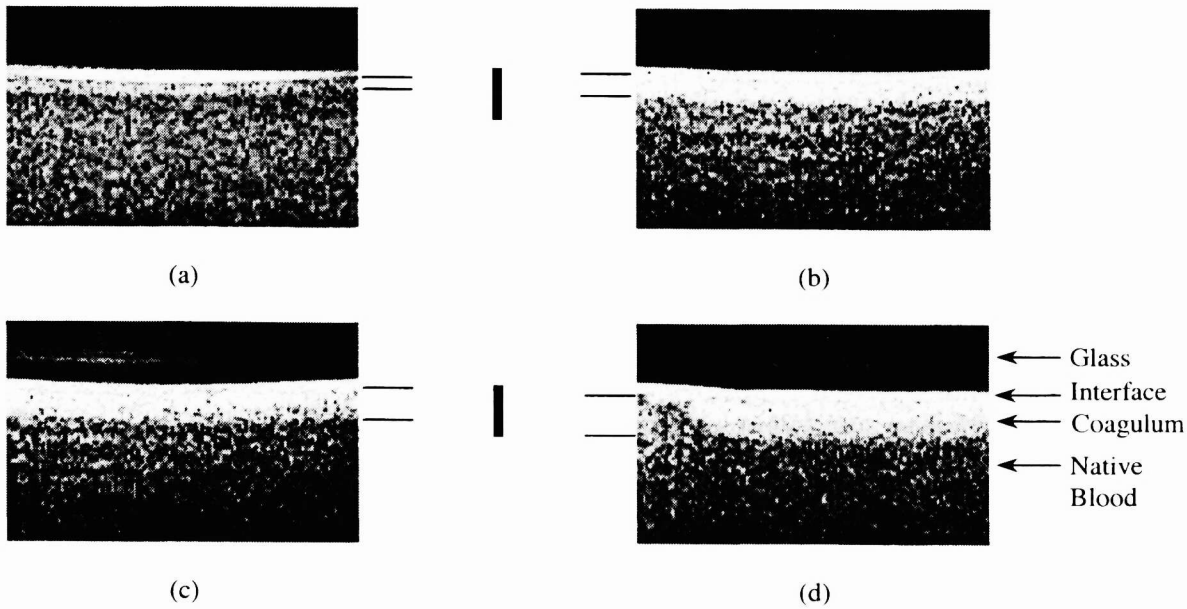

Figure 4: OCT images documenting the morphology of coagulated regions of whole blood at radiant exposures of (a) 4.4, (b) 6, (c) 8, and (d) 10 J/cm^2. As labeled in (d), four regions are visible (from top to bottom): glass (black), glass-blood interface (white), coagulated blood (bright speckle) and native blood (darker speckle). Size bars represent a distance of 200 μm. Approximate thickness of each coagulum is indicated by a pair of thin lines. The left side of image (d) shows edge of coagulum. Note that the intensity of the OCT signal in (a) is lower in the coagulum (and higher in the native blood) than in the corresponding regions of the other images.

3.4 Transmission measurements

The traces recorded by the oscilloscope indicated a stable pre-irradiation transmission level, followed by a large increase in transmission due to stray light from the KTP laser flashlamp, and a post-pulse transmission level. The change in transmission (pre- to post- laser pulse) with increasing radiant exposure is presented in Figure 5. Six or more samples were used for each point in the graph. At low radiant exposures, the difference in transmission before and after the laser pulse was insignificant. As H_o increased from 4.0 to 5.0 J/cm^2, a sharp decrease in transmission occurred. For radiant exposures greater than 5.0 J/cm^2 the transmission decrease became approximately linear with radiant exposure.

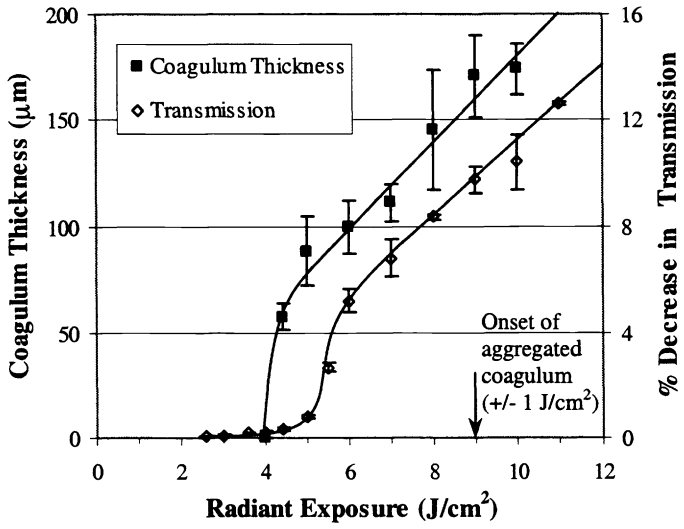

Figure 5: The effect of increasing radiant exposure on coagulum thickness (from OCT images) and change in transmission of co-aligned laser beam (λ = 635 nm). Curve fits are arbitrary.

4. DISCUSSION

4.1 Threshold radiant exposure for coagulation

By definition, coagulation involves thermally-induced alteration of 63% or more of the cells or molecules. In most experimental studies it is assumed that coagulation corresponds to visually-observable and optically-detectable alterations in tissue (such as the whitening of albumen). In the present study, different methods indicated a variety of threshold radiant exposures between 3.6 and 5.0 J/cm^2: (1) visual observation, 3.6 J/cm^2; (2) transmission measurements, ~4.0 J/cm^2; (3) optical coherence tomography, 4.4 J/cm^2; and (4) the Arrhenius calculations for Hb, 5.0 J/cm^2. The values from the three experimental techniques are based on the lowest radiant exposure at which significant coagulation-induced changes became evident. The fourth method involved indirect theoretical evaluation of the concentration of damage molecules.

This lack of agreement between the results may be due to the fact that blood is a non-homogeneous medium comprised of various proteins which have different coagulation thresholds and/or that concentrations of thermal damage less than that required for coagulation may be detectable. It is possible that initial changes in visual appearance and transmission may have been a result of scattering brought on by denaturation of erythrocyte membrane proteins that are not as thermally-tolerant as other blood constituents.[7] For a radiant exposure of 4.4 J/cm^2, the Arrhenius calculations indicated that approximately 10% of Hb molecules were damaged (Ω = 0.1). The small difference in signal intensity between the coagulum and native blood in Figure 4a (H_o = 4.4 J/cm^2) as compared to the differences noted for higher radiant exposures may also indicate a level of damage significantly less than 63%. Therefore, the threshold radiant exposure for coagulation is likely between 4.4 and 5.0 J/cm^2, and will be approximated as 4.7 J/cm^2.

It should be noted that the discrepancy between the thermal damage level predicted for radiant exposures between 4.4 and 5.0 J/cm^2 (for Hb) and the ideal value of 1.0 may be due to temperature measurement error, error in the rate process

coefficients, or the use of the wrong rate process coefficients (perhaps the onset of coagulation is dominated by albumin denaturation which, as Figure 1 indicates, has a slightly lower threshold temperature than Hb).

A previous study by Verkruysse *et al.*[14] indicated that for *in vitro* irradiation of blood with a 0.5 ms laser pulse (λ = 586 nm), coagulation onset occurs when a radiant exposure corresponding to H_{th} has been delivered. This approach does not appear to be completely valid for the parameters in the present study. A radiant exposure equivalent to H_{th} was delivered for the 8, 10 and 12 J/cm^2 pulses in 5.9, 4.7 and 3.9 seconds, respectively (assuming a constant irradiance), and resulted in temperatures of 93.7, 94.7, and 103.1 °C and thermal damage levels of 0.1, 0.1, and 2.1 (at the respective times). Although the difference between the damage levels may not be highly significant, this data does provide some evidence that longer exposure durations resulted in greater thermal losses, which in turn led to reduced temperatures and damage. The discrepancy between these results and that of Verkruysse *et al.* is likely due to differences in pulse duration and blood absorption which directly affect the level of thermal confinement.

4.2 Threshold temperatures for coagulation

By definition, a threshold temperature (T_{th}) involves step changes in temperature and well-defined exposure times.[19] Highly transient laser processes do not satisfy either of these ideal conditions. Therefore, it is more useful to define two alternate threshold temperatures: an onset threshold temperature (T_{on}) - the maximum temperature that occurs for the threshold radiant exposure for coagulation, and a transient threshold (T_{tr}) - the transient temperature at which coagulation occurs during a laser pulse for which the radiant exposure is significantly greater than H_{th}.

Interpolating from the data in Figure 2, the threshold radiant exposure of 4.7 J/cm^2 corresponds to a maximum radiometric temperature of 93 +/- 3 °C (T_{on}). This result is in reasonable agreement with the threshold temperatures for exposure durations of 10 ms for blood constituents such as hemoglobin and albumin (Table 1), but significantly higher than the 60 to 70 °C used to predict vessel necrosis in theoretical models of pulsed laser treatment of vascular lesions.[21,22,24]

For radiant exposures significantly greater than H_{th}, T_{on} is reached during the laser pulse, but since coagulation at T_{on} requires an exposure duration of several milliseconds, greater temperatures (and a greater damage accumulation rate) are produced before coagulation occurs (at T_{tr}). Since transmission and coagulum thickness data were not collected during the laser pulse, it is difficult to directly identify T_{tr} from experimental results. However, Figure 3b indicates that coagulation onset for H_o = 8.0, 10.0 and 12.0 J/cm^2 occurred at nearly identical temperatures (99.0, 101.0, and 99.1 °C). The predictions of coagulation onset (Figure 3b) appear to be consistent with the transition from a decreasing rate of temperature rise to one which is constant (Figure 2), an effect which may reflect the coagulation-induced changes in light scattering (as discussed further in Section 4.4). Thus, it is likely that the transient threshold temperature (T_{tr}) is approximately 100 °C.

4.3 The Arrhenius equation

Threshold temperatures are useful for rough approximations of damage onset. However, the Arrhenius equation provides a method of quantifying thermal damage accumulation which is much more accurate and flexible. The cost of these benefits is that calculation of thermal damage at any specific location requires accurate time-temperature data (particularly for temperatures close to threshold temperatures). Although a logarithmic scale such as that used in Figure 3 is useful to understand the time-temperature relationship of thermal damage, it also can be misleading. The most important changes in thermal damage occur near the coagulation damage threshold, with Ω values of 0.1, 1.0, and 10.0 corresponding to damage concentrations of 9.5%, 63.2% and 99.995% , respectively.

The data in Figure 3 indicates that the accuracy of the Arrhenius relation is highly dependent upon the rate process coefficients used. The final thermal damage for H_o = 4.7 J/cm^2 using Hb and bulk skin coefficients were calculated to be are 0.32 and 10^6, respectively (from the Arrhenius equation and temperatures interpolated from the experimental data for H_o = 4.0 and 5.0 J/cm^2). The Arrhenius calculations using published data for Hb indicate much better agreement with the experimental results than do the calculations employing bulk skin data.

It should be noted that the time-temperature relationship indicated by most of the rate process parameters in Table 1 are quite similar. The similarity of the threshold values for hemoglobin, albumin, and arterial tissue - each potentially significant components in photothermolysis - indicates that coagulation of blood and arterial tissue may occur nearly simultaneously, and thus work together to destroy vessels.

4.4 Thermal damage-induced light scattering

The rate of change in coagulum thickness with H_o was large for H_o = 4.0-5.0 J/cm^2, whereas the corresponding changes in transmission were minimal. One possible explanation for this apparent discrepancy is that the coagulum has scattering parameters similar to that of coagulated albumin (μ_s ~ 150 cm^{-1}, g = 0.8),[25] and thus for a coagulum thickness less than ~67 μm it is probable that a photon undergoes a single forward-scattering event, whereas a thicker coagulum results in multiple scattering events which significantly alter a photon's trajectory. Another possible mechanism – one which relates to the arguments presented in the previous section - is that for radiant exposures near H_o = 4.4 J/cm^2 the percentage of molecules which are denatured is closer to 9.8% than 100%, and the scattering coefficient is proportionally less than the value quoted above.

For radiant exposures above 5.0 J/cm^2, Figure 2 indicates that the rate of temperature rise eventually became nearly constant towards the end of the laser pulse. This effect appears to have occurred near 100 °C, and was nearly simultaneous with the onset of coagulation as predicted by the Arrhenius relation using the rate process coefficients of hemoglobin as seen in Figure 3. Therefore, it is likely that it was a result of a dynamic increase in scattering due to coagulation.

Although a dynamic decrease in transmission was been noted by Verkryusse *et al.*[14] during laser irradiation of blood (at λ = 586 nm), the authors' concluded that the change was due to changes in absorption rather than scattering. At wavelengths for which there is a large disparity in absorption between Hb and HbO_2, significant transmission changes may result from thermally-induced deoxygenation of HbO_2.[13] However, since the difference between μ_a for Hb (185.1 cm^{-1}) and HbO_2 (228.8 cm^{-1}) is less than 20% at λ = 532 nm, it is not likely that this effect was significant in the measurements presented in this study.[30] Other investigations are in agreement with our findings that thermal damage of blood constituents results in a significant increase in scattering.[13,16]

4.5 Coagulum size and consistency

The variation in coagulum thickness with radiant exposure (Figure 5) shows a large initial slope followed by a more moderate slope which continues until ablation. The second phase of the curve indicates a region for which changes in coagulum depth occur in nearly direct proportion to changes in radiant exposure. Similar trends have been noted in previous studies of Holmium:YAG irradiation of albumen.[15,16] As shown in Figure 5, the maximum blood coagulum thickness recorded was 175 μm (H_o = 10 J/cm^2). If data is extrapolated to H_o = 12 J/cm^2, the maximum achievable thickness without inducing ablation would be approximately 200 μm. This suggests that full lumen coagulation of blood would require a vessel of less than 400 μm in diameter, assuming the vessel is irradiated by diffuse light.

The penetration depth of 532 nm light in oxygenated blood is ~45 μm.[30] At a depth of 175 μm, only 1.8% of the initial fluence remains if the blood is highly oxygenated (3.9% if de-oxygenated). Therefore, it is likely that axial heat diffusion causes the coaguled region to be thicker than would be possible if the laser pulse were shorter and the process thermally confined. It is also possible that convective (pressure or temperature-driven) flow may play a role.

The transition from a region of disconnected (or weakly bonded), denatured proteins to an aggregated coagulum appears to have taken place between radiant exposures of 8.0 and 10.0 J/cm^2. If a threshold radiant exposure for aggregation of 9.0 J/cm^2 is assumed, the threshold temperature would be ~115 °C, and the resulting thermal damage, ~1000 (for Hb). Although the use of a threshold thermal damage may be a useful approximation, no direct correlation between Ω and coagulum strength has been established (and no delineation between aggregated and non-aggregated sections was observed in OCT images). Alternatively, it may be necessary to determine a new set of rate process coefficients in order to accurately model this effect. The higher aggregation threshold suggests that the largest vessel that could be filled with a coagulum would have a diameter far less than 400 μm.

The finding of blood coagula in various stages of aggregation corresponding to radiant exposure level is in agreement with findings by Barton *et al.*[31] which indicated that the threshold for embolized coagulum formation was much lower than that required for formation of a flow-stopping coagulum. The mechanism of transition from an unconnected solution of denatured molecules to a strongly bonded coagulum is very significant not only for arresting flow in blood vessels but for other applications such as forming patent anastomoses with a laser, yet it is still not well understood. It is likely that the primary mechanism is either (1) an increase in the concentration of denatured molecules due to additional thermal damage or (2) evaporative water loss which decreases the inter-molecular space, thus facilitating bond formation. In order to achieve a

better understanding of this process, it will be necessary to study the molecular composition and microscopic morphology of coagula.

4.6 Effect of water vaporization

The thermal camera data provides evidence of several significant dynamic mechanisms. In Figure 2, the linear slope for the lowest radiant exposure indicates a situation in which minimal dynamic changes occurred. As H_o increased and temperatures rose above 70 °C, a decrease in the rate of temperature rise resulted. This was coincident with the observation of vapor production. These results indicate that heat losses to phase change became significant at about 70 °C, leading to a decrease in the rate of temperature rise. This is in fair agreement with the literature which indicates that for CW processes, the evaporation becomes significant at 60 °C, and increases exponentially with temperature.[32,33]

The results indicate that the threshold radiant exposure for ablation was ~12 J/cm^2 and that the corresponding maximum surface temperature (during non-ablative irradiation) was 145 °C. In order to establish the maximum tissue temperature, it is necessary to consider two possible scenarios proposed in the literature: (1) Evaporative cooling acted to moderate the rate of temperature increase at temperatures above 60 °C. As the tissue became desiccated - likely near 100 °C - the cooling mechanism was reduced and the rate of temperature rise increased sharply, leading to ablation.[19] This raises the question of whether the change in rate of temperature rise near 100 °C (Figure 2) was at least partially due to desiccation. If this description of the ablation process is accurate, then the surface temperature was also the maximum tissue temperature. (2) Alternatively, surface heat loss and a layer of highly scattering coagulum may have produced a subsurface temperature peak which in turn led to phase change and a corresponding subsurface peak in pressure. When internal pressures exceeded the restraining forces (eg. blood surface tension, coagulum tensile strength), ablation occurred.[34] If this scenario is accurate, then the maximum temperature may have been significantly greater than 145 °C. The remaining questions indicate a more thorough investigation is necessary to elucidate vaporization-related mechanisms and effects.

4.7 Implications for theoretical modeling

The most obvious implication for theoretical modeling of coagulation is that a full Arrhenius equation solution with appropriate rate process coefficients provides the most accurate prediction of coagulation. However, if threshold radiant exposures or temperatures are used, they should be consistent with the Arrhenius time-temperature relationship. For coagulation of whole blood by a 10 ms KTP laser pulse, one should be careful to discern between the onset threshold temperature (T_{on} ~ 93 °C) and the transient threshold temperature (T_{tr} ~ 100 °C).

As discussed above, coagulation onset as predicted by the Arrhenius equation may not be an appropriate endpoint for many applications which require an aggregated coagulum. In order to compensate for this difference, it may be useful to employ an approximate threshold thermal damage (Ω) value of 1000 (rather than 1.0). Additionally, ablation may not occur until temperatures of 145 °C (or greater) are reached. Therefore, numerical predictions of non-ablative events in which blood reaches temperatures well in excess of 100 °C should not be considered unreasonable.

The results of this study indicate that several modifications of common modeling practices may result in an improvement of the predictive ability of these models. The primary dynamic effects appeared to be related to the enthalpy of phase change and coagulation-induced scattering. The former has been modeled using the assumption that phase change occurs at 100 °C[35] and for non-isothermal evaporation at a free surface[33], whereas the latter has been modeled using an iterative optical-thermal technique which accounts for dynamic changes in scattering as a gradual effect proportional to the concentration of thermally altered molecules.[36]

5. CONCLUSIONS

In this study, pulsed laser-induced coagulation of blood have been investigated quantitatively using high-speed thermal imaging, optical coherence tomography, transmission measurements, and Arrhenius equation-based calculations. The results indicate that for irradiation of whole blood *in vitro* by a KTP laser (λ = 532 nm, τ_p = 10 ms):

(1) *Coagulation mechanisms and effects*: The threshold radiant exposure for coagulation onset is 4.4-5.0 J/cm^2; threshold temperatures for coagulation are 90-100 °C; the threshold radiant exposure for formation of an aggregated coagulum is ~9 J/cm^2; thermal coagulation induces a significant increase in light scattering; the maximum coagulation thickness that can be achieved is less than 200 μm; and the primary component of the coagulum is likely hemoglobin.

(2) *Arrhenius equation*: The Arrhenius equation is valid (given that appropriate rate process coefficients are used) and the most accurate way of predicting coagulation onset; the rate process coefficients of hemoglobin are more accurate in predicting thermal damage in blood than are the coefficients for bulk skin.
(3) *Vaporization mechanisms and effects*: evaporative heat loss becomes significant for temperatures greater than ~70 °C; the maximum surface temperature that can be reached without inducing ablation is 145 °C; and the threshold radiant exposure for ablation is ~12 J/cm^2.

The results of this study have helped to increase our understanding of the mechanisms of laser-induced coagulation of whole blood in a quantitative way. They should be useful in improving and verifying numerical models, and in increasing the effectiveness of therapeutic laser treatments which involve coagulation of blood constituents.

ACKNOWLEDGMENTS

The authors would like to acknowledge Dr. Jennifer Barton, Dr. James Lepock, Dr. John Pearce, Dr. R. Rox Anderson, and Dr. Martin van Gemert for significant discussions which have benefited this study. Funding for this research was provided in part by grants from the Air Force Office of Scientific Research through MURI from DDR&E (F49620-98-1-0480), the Office of Naval Research Free Electron Laser Biomedical Science Program (N00014-91-J-1564), and the Albert W. and Clemmie A. Caster Foundation. A. J. Welch is the Marion E. Forsman Professor of Electrical and Computer Engineering.

REFERENCES

1. M. J. C. van Gemert, A. J. Welch, J. W. Pickering, and O. T. Tan, "Laser treatment of port wine stains," in *Optical-Thermal Response of Laser-Irradiated Tissue*, A. J. Welch and M. J. C. van Gemert, eds., Plenum Press, New York, 1995.
2. D. P. Poppas, E. J. Wright, P. D. Guthrie, L. T. Shlahet, and A. B. Retik, "Human albumin solders for clinical application during laser tissue welding," *Lasers Surg. Med.* **19**, pp. 2-8, 1996.
3. J. K. Barton, J. A. Izatt, and A. J. Welch, "Investigating pulsed dye laser-blood vessel interaction with color Doppler optical coherence tomography," *Optics Express (http://epubs.osa.org/opticsexpress)* **2**, pp. 251-256, 1998.
4. J. K. Barton, D. X. Hammer, T. J. Pfefer, D. J. Lund, B. E. Stuck, and A. J. Welch, "Simultaneous irradiation and imaging of blood vessels during pulsed laser delivery," *Lasers Surg. Med., in press.*
5. A. C. Guyton, *Textbook of medical physiology*, W. B. Saunders Co., Philadelphia, 1991.
6. W. Kapit, R. I. Macey, and E. Meisami, *Physiology coloring book*, Harper Collins, Cambridge, 1987.
7. A. M. K. Nilsson, G. W. Lucassen, W. Verkruysse, S. Andersson-Engels, and M. J. C. van Gemert, "Changes in optical properties of human whole blood *in vitro* due to slow heating," *Photochem. Photobiol.* **65**, pp. 366-373, 1997.
8. G. S. Abela, F. Crea, W. Smith, C. J. Pepine, and C. R. Conti, "*In vitro* effects of argon laser radiation on blood: quantitative and morphologic analysis," *J. Am. Coll. Cardiol.* **5**, pp. 231-237, 1985.
9. S. Thomsen, "Pathologic analysis of photothermal and photomechanical effects of laser-tissue interactions," *Photochem. Photobiol.* **53**, pp. 825-835, 1991.
10. J. R. Lepock, H. E. Frey, H. Bayne, and J. Markus, "Relationship of hyperthermia-induced hemolysis of human erythrocytes to the thermal denaturation of membrane proteins," *Biochim. Biophys. Acta* **980**, pp. 191-201, 1989.
11. J. H. Theis, G. Lee, R. M. Ikeda, D. Stobbe, C. Ogata, H. Lui, and D. T. Mason, "Effects of laser irradiation on human erythrocytes: considerations concerning clinical laser angioplasty," *Clin. Cardiol.* **6**, pp. 396-398, 1983.
12. S. Flock, L. Smith, and M. Waner, "Quantifying the effects on blood of irradiation with four different vascular-lesion lasers, " *Proc. SPIE* **1882**, pp. 237-242, 1993.
13. T. Halldorsson, "Alteration of optical and thermal properties of blood by Nd:YAG laser irradiation," *The 4th Congress of The International Society for Laser Surgery*, 1981.
14. W. Verkruysse, A. M. K. Nilsson, T. E. Milner, J. F. Beek, G. W. Lucassen, and M. J. C. van Gemert, "Optical absorption of blood depends on temperature during a 0.5 ms laser pulse at 586 nm," *Photochem. Photobiol.* **67**, pp. 276-281, 1998.
15. T. Asshauer, G. P. Delacretaz, S. Rastegar, "Photothermal denaturation of egg white by pulsed holmium laser," *Proc. SPIE* **2681**, pp. 120-124, 1996.
16. T. J. Pfefer, K. F. Chan, D. X. Hammer, and A. J. Welch, "Pulsed holmium:YAG-induced thermal damage in albumen," *Proc. SPIE* **3254**, pp. 192-202, 1998.

17. F. C. Henriques, Jr. and A. R. Moritz, "Studies in thermal injury I. The conduction of heat to and through skin and the temperature attained therein. A theoretical and an experimental investigation," *Am. J. Pathol.* **23**, pp. 531-549, 1947.
18. A. R. Moritz and F. C. Henriques, Jr., "Studies in thermal injury II. The relative importance of time and surface temperature in the causation of cutaneous burns," *Am. J. Pathol.* **23**, pp. 695-720, 1947.
19. J. Pearce and S. Thomsen, "Rate Process Analysis of Thermal Damage," in *Optical-Thermal Response of Laser-Irradiated Tissue*, A. J. Welch and M. J. C. van Gemert, eds., Plenum Press, New York, 1995.
20. Y. Yang, A. J. Welch, and H. G. Rylander, "Rate process parameters of albumen," *Lasers Surg. Med.* **11**, pp. 188-190, 1991.
21. D. J. Smithies, P. H. Butler, W. A. Day, and E. P. Walker, "The effect of the illumination time when treating port-wine stains," *Las. Med. Sci.* **10**, pp. 93-104, 1995.
22. J. F. de Boer, G. W. Lucassen, W. Verkruysse, and M. J. C. van Gemert, "Thermolysis of port-wine-stain blood vessels: diameter of a damaged blood vessel depends on the laser pulse length," *Las. Med. Sci.* **11**, pp. 177-180, 1996.
23. C. Sturesson and S. Andersson-Engels, "Mathematical modelling of dynamic cooling and pre-heating used to increase the depth of selective damage to blood vessels in laser treatment of port wine stains," *Phys. Med. Biol.* **41**, pp. 413-428, 1996.
24. M. J. C. van Gemert, A. J. Welch, I. D. Miller, and O. T. Tan, "Can physical modeling lead to an optimal laser treatment strategy for port-wine stains?," in *Laser Applications in Medicine and Biology*, Wolbarsht M. L., eds. New York: Plenum Press, 1991.
25. K. M. McNally, "Optical and thermal studies of laser-solder tissue repair *in vitro*," Ph.D. Dissertation, School of Mathematics, Physics, Computing and Electronics, Macquarie University, Australia, 1998.
26. N. A. Moussa, E. N. Tell, and E. G. Cravalho, "Time progression of hemolysis of erythrocyte populations exposed to supraphysiological temperatures," *J. Biomech. Eng.* **101**, pp. 213-217, 1979.
27. F. S. Barnes, "Biological damage resulting from thermal pulses," in *Laser Applications in Medicine and Biology*, M. L. Wolbarsht, ed., Plenum Press, New York, 1974.
28. R. Agah, J A Pearce, A J. Welch, and M. Motamedi, "Rate process model for arterial tissue thermal damage: implications for vessel photocoagulation," *Lasers Surg. Med.* **15**, pp. 176-184, 1994.
29. J. K. Barton, T. E. Milner, T. J. Pfefer, J. S. Nelson, and A. J. Welch, "Optical low-coherence reflectometry to enhance Monte Carlo modeling of skin," *J. Biomed. Opt.* **2**, pp. 226-234, 1997.
30. W. G. Zijlstra, A. Buursma, and W. P. Meeuwsen-van der Roest, "Absorption spectra of human fetal and adult oxyhemoglobin, de-oxyhemoglobin, carboxyhemoglobin, and methemoglobin," *Clin. Chem.*, **37**, pp. 1633-1638, 1991.
31. J. K. Barton, "Predicting dosimetry for laser coagulation of *in vivo* cutaneous blood vessels," Ph. D. Dissertation, The University of Texas at Austin, August, 1998.
32. F. P. Incropera and D. P. DeWitt, *Fundamentals of Heat and Mass Transfer,* Fourth Edition, John Wiley and Sons, New York, 1996.
33. J. H. Torres, M. Motamedi, J. A. Pearce, and A. J. Welch, "Experimental evaluation of mathematical models for predicting the thermal response of tissue to laser irradiation," *Appl. Opt.* **32**, pp. 597-606, 1993.
34. G. L. LeCarpentier, M. Motamedi, L. P. McMath, S. Rastegar, and A. J. Welch, "Continuous wave laser ablation of tissue: analysis of thermal and mechanical events," *IEEE Trans. Biomed. Eng.* **40** (2), pp. 188-199, 1993.
35. A. Sagi, A Avidor-Zehavi, A Shitzer, M Gerstmann, S Akselrod, and A Katzir, "Heating of biologial tissue by laser irradiation: temperature distribution during laser ablation," *Opt. Eng.* **31**, pp. 1425-1431, 1992.
36. S. Rastegar, B. M. Kim, and S. L. Jacques, "Role of temperature dependence of optical properties in laser irradiation of biological tissue, " *Proc. SPIE* **1646**, pp. 228-231, 1992.